

Double-period breathers in a driven and damped lattice

G. Bel,^{1,2} B. S. Alexandrov,³ A. R. Bishop,³ and K. Ø. Rasmussen³

¹*Department of Solar Energy and Environmental Physics, Blaustein Institutes for Desert Research and Department of Physics, Ben-Gurion University of the Negev, Sede Boqer Campus 84990, Israel*

²*Center for Nonlinear Studies (CNLS), Los Alamos National Laboratory, Los Alamos, New Mexico 87545, USA*

³*Theoretical Division, Los Alamos National Laboratory, Los Alamos, New Mexico 87545, USA*



(Received 7 September 2018; published 10 December 2018)

Spatially localized and temporally oscillating solutions, known as discrete breathers, have been experimentally and theoretically discovered in many physical systems. Here, we consider a lattice of coupled damped and driven Helmholtz-Duffing oscillators in which we found a spatial coexistence of oscillating solutions with different frequencies. Specifically, we demonstrate that stable period-doubled solutions coexist with solutions oscillating at the frequency of the driving force. Such solutions represent period-doubled breathers resulting from a stability overlap between subharmonic and harmonic solutions and exist up to a certain strength of the lattice coupling. Our findings suggest that this phenomenon can occur in any driven lattice where the nonlinearity admits bistability (or multi-stability) of subharmonic and harmonic solutions.

DOI: [10.1103/PhysRevE.98.062205](https://doi.org/10.1103/PhysRevE.98.062205)

Discrete breathers (DBs) are solutions to nonlinear lattice systems that periodically oscillate in time and are exponentially localized in space [1]. Discrete breathers have been studied theoretically and experimentally in a multitude of settings, involving a wide array of physical mechanisms [2]. DBs have been demonstrated experimentally and theoretically in studies of ordered granular chains [3,4], as well as in nonlinear, locally resonant magnetic metamaterials [5] and systems of electromechanical resonators [6]. While discrete breathers share many traits with solitons, they stand out because of their localization brought about by a specific sensitivity to lattice discreteness. Although dissipation and driving are typically key experimental features, there are limited theoretical and numerical studies of DBs [7] that include such effects.

Here we study a generic type of discrete breather solutions that exist in the presence of both driving and damping and take direct advantage of the intrinsic nonlinear phenomena of period doubling. To the best of our knowledge, these subharmonic breathers were first recognized in studies of the nonlinear dynamics of double-stranded DNA [8,9] and subsequently also explored in experimental and numerical studies of periodically driven and damped chains of pendula [10–12]. Here we chose a minimal model to elucidate the phenomena of subharmonic breathers. We show that, similar to more traditional DBs, oscillations with half the frequency (double period) of the driving force can be maintained in a localized region of a lattice (of oscillators) oscillating at the frequency of the driving force.

As is well understood, period doubling occurs through a bifurcation in a dynamical system in which a slight change in a parameter value in the system's equations leads to switching to a new behavior with twice the period of the original system [13,14]. A periodically driven nonlinear oscillator typically responds with solutions that oscillate at the same frequency as the periodic drive. In such systems, a period-doubling bifurcation is expressed through these solutions losing stability as

solutions oscillating at half the driving frequency gain stability. One of the simplest examples of a system that exhibits this behavior is the driven and damped Helmholtz-Duffing oscillator. This model was used in various systems including logic devices [15,16] and neural networks [17,18]. The dynamics of the Helmholtz-Duffing oscillator is described by

$$\frac{d^2y}{dt^2} + y + y^3 + by^2 + \gamma \frac{dy}{dt} = f \cos(\omega_0 t), \quad (1)$$

where b is a tunable coefficient dictating the asymmetry of the anharmonic potential, γ is the damping coefficient, and f and ω_0 are the strength and frequency of the periodic drive, respectively. If nothing else is noted, we use the following values for these parameters throughout this paper: $b = 0.5$, $\gamma = 0.2$, and $\omega_0 = 1$. We vary the strength of the driving force, f , as the bifurcation parameter, but the frequency ω_0 could have been used in a similar manner. Figure 1 shows a typical bifurcation diagram for the driven and damped Helmholtz-Duffing oscillator (the bifurcation diagram was derived using the AUTO numerical continuation program [19]). As expected, Fig. 1 shows that for small values of the driving force, f , the stable solution of Eq. (1) possesses the frequency and period of the driving force. However, at $f \simeq 9$, these solutions lose stability, while solutions with half the frequency (double period) of the drive emerge and are stable. These double-period solutions similarly lose stability at $f \simeq 11$ where quadrupled-period solutions (not shown) exist. For even larger values of f , this scenario reverses, and stable solutions with frequency ω_0 and $\omega_0/2$ can be seen to emerge. As a result, in the range $13 < f < 14$, it can be observed that both the ω_0 and $\omega_0/2$ solutions are stable. Figure 2 shows examples of these two stable solutions for $f = 13.3$. We also investigated the bifurcation diagrams for different driving frequencies; albeit more complicated, the same type of bistability can be found for a wide range of driving frequencies. Moreover, the amplitudes of the $1T$ and $2T$ solutions are

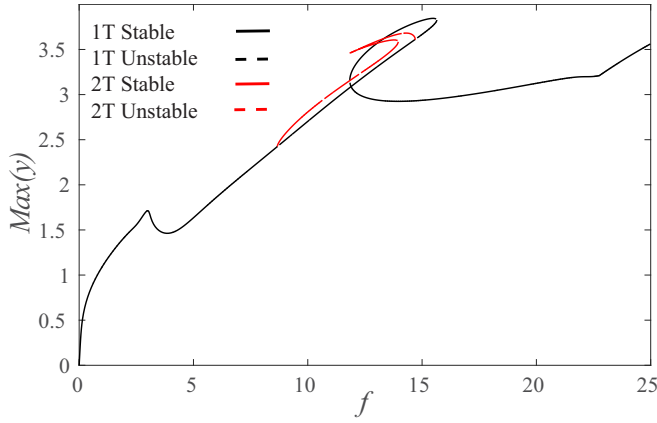


FIG. 1. The bifurcation diagram of Eq. (1). The solid (dashed) lines represent (un)stable solutions. The black lines correspond to solutions with the same period as the driving force ($T = 2\pi/\omega_0$) while the red (color online) lines correspond to solutions with the doubled period. It should be noted that this is not the complete bifurcation diagram for this range of values of f , as there are additional branches of stable quadrupled period solutions, etc. The parameters used in this bifurcation diagram are $b = 0.5$, $\gamma = 0.2$, and $\omega_0 = 1$.

not very different for all the driving frequencies we explored. Similarly, we found that varying the values of the friction and the asymmetry parameters of the model does not broaden the bistability range significantly nor does it change much the difference between the amplitudes of the $1T$ and $2T$ solutions.

The existence of the two types of solutions is not new, and the double-period bifurcation was extensively investigated (e.g., Ref. [14]). However, much less attention was given to the bistability of the solutions and to their possible coexistence. The latter is of particular interest in a system of coupled driven oscillators. In this context, a natural generalization of the single Helmholtz-Duffing oscillator considered above is

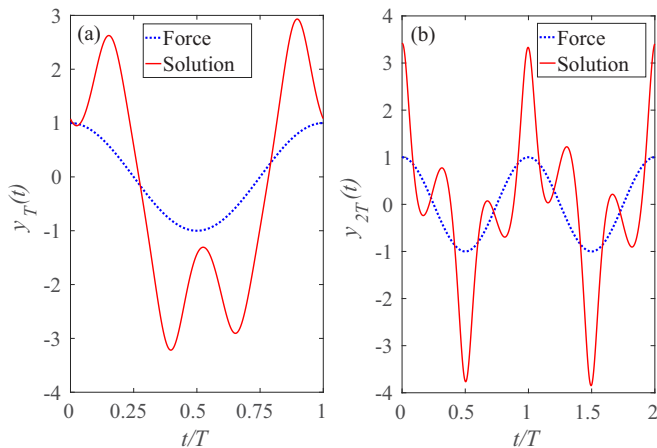


FIG. 2. (a) y_T , the solution (solid red line) with the same frequency as the driving force, and (b) y_{2T} , the period-doubled solution (solid red line). For clarity, both panels also show (dotted blue lines) the driving force. The parameters are the same as in Fig. 1 with $f = 13.3$ (corresponding to a value within the bistability range of the two solutions).

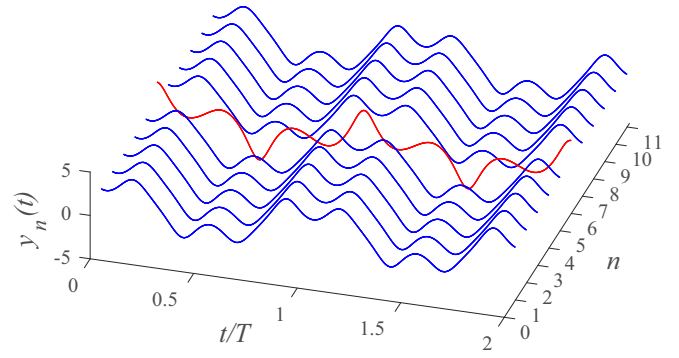


FIG. 3. The solutions of coupled driven oscillators with periodic boundary conditions. The middle oscillator oscillates with a doubled period while the other oscillators have the same frequency as the driving force. The parameters are the same as in Fig. 2 with $c = 0.1$.

a discrete chain of coupled oscillators whose dynamics is described by the following equation:

$$\frac{d^2 y_n}{dt^2} = -y_n - y_n^3 - b y_n^2 - \gamma \frac{dy_n}{dt} + c(y_{n-1} - 2y_n + y_{n+1}) + f \cos(\omega_0 t), \quad n = 1, 2, \dots, N-1, N. \quad (2)$$

The first three terms on the right hand side describe the force resulting from the asymmetric potential (the coefficient b can be thought of as controlling the degree of asymmetry), the fourth term describes the friction (with a friction coefficient γ), the fifth term describes the linear coupling to the nearest neighbors, and the last term describes the periodic driving force. The equation is supplemented by the periodic boundary conditions

$$\begin{aligned} y_{N+1} &= y_1, \\ y_0 &= y_N. \end{aligned} \quad (3)$$

In what follows, we use the same parameters we used earlier for the potential of each oscillator and different values for the coupling strength, c . In Fig. 3, we show a stable solution of a system of $N = 11$ coupled oscillators. The plane axes correspond to the time (in units of the driving force period, T) and to the number of the oscillator, n . The vertical axis corresponds to the value of the variable, $y_n(t)$, during two periods of the driving force. This solution demonstrates the coexistence of a period-doubled solution (for $n = 6$, red line) and the driving period solutions (for all other n 's, blue lines). The coupling strength for the presented solution is $c = 0.1$.

To better illustrate the fact that two different solutions coexist, we depict in Fig. 4 the power spectra of the coupled oscillators. The middle oscillator ($n = 6$) shows peaks at $\omega_0/2$ and odd and even integer multiples of this frequency (corresponding to double the period of the driving force), while all the other oscillators (only $n = 1$ and $n = 5$ are shown for clarity) only show peaks for ω_0 and integer multiples of it.

The stable solution shown above could be reached by starting with a system in which the middle oscillator oscillates with double the period of the driving force and all other oscillators oscillate with the period of the driving force. In this case, the initial condition is such that the middle oscillator is

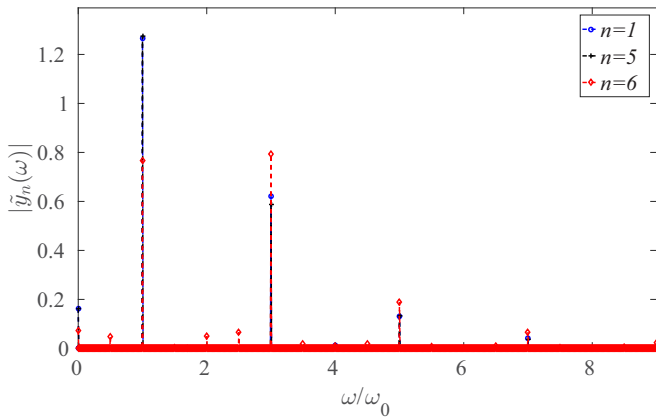


FIG. 4. The power spectra of coupled oscillators. The middle oscillator ($n = 6$) shows peaks at $\omega_0/2$ and some odd multiples of this frequency while the others (only $n = 5$ and $n = 1$ are shown) only show peaks at integer multiples of ω_0 . The parameters are the same as in Fig. 3.

driven with only one frequency, the frequency of the driving force. The neighbors of the middle oscillator are driven by two different frequencies, the strong external driving force and the weaker driving with the doubled period due to the coupling to the middle oscillator. However, due to the fact that the force exerted by the neighbors is much weaker than the external one, the system converges to a stable solution of coexisting frequencies. An initial state in which the middle oscillator oscillates with the frequency of the driving force and all the others with half the frequency is not stable under the same strength of the coupling (c) coefficient. Starting from this latter initial state, while keeping all the parameters of the system the same, resulted in a complicated stable solution in which some of the oscillators show a non-monochromatic spectrum. The stable solution for this initial condition is shown in Fig. 5.

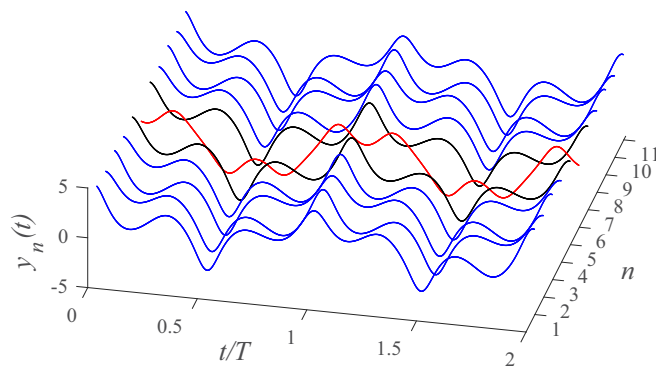


FIG. 5. The solutions of coupled driven oscillators with periodic boundary conditions. Initially, the middle oscillator oscillates with the period of the driving force while all other oscillators have a doubled period. The parameters are the same as in Fig. 3. In this case, the initial state is not stable because the middle oscillator is driven by both the external force with period $T = 2\pi/\omega_0$ and the force exerted by the neighbors with period $2T$.

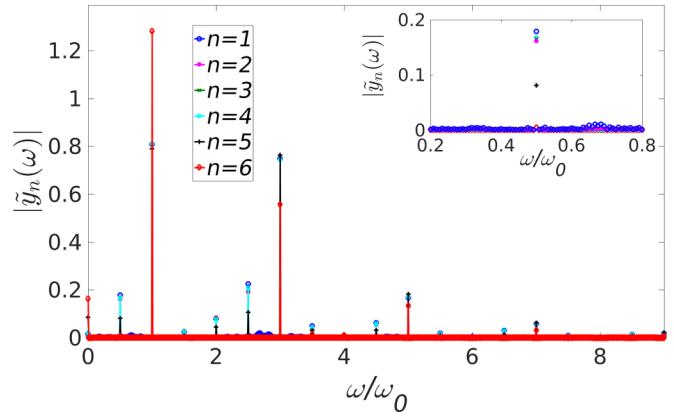


FIG. 6. The power spectra of coupled oscillators for the solution shown in Fig. 5. The stronger deviation from monochromatic driving results in more complicated spectra.

The nature of this complex solution is better seen by investigating the power spectra of the individual oscillators. The spectra are shown in Fig. 6. As can be seen, the oscillators show several peaks and additional contributions at non-integer multiples of the driving period. For weaker coupling between the oscillators, a solution, in which one oscillator has the driving period and all others have the double period, is also stable.

The result shown above focused on the case of moderate coupling between the oscillators; i.e., the coupling coefficient was set to $c = 0.1$. For stronger coupling, the oscillators tend to oscillate with the same frequency and phase. In Fig. 7, we depict the solution for the case of a stronger coupling, $c = 1$. In this case, despite the initial condition in which the middle oscillator has the doubled period and the others the same period as the driving force, the stable solution is such that all the oscillators have the frequency of the driving force.

It is important to note that for strong coupling between the oscillators, any mixed initial condition (i.e., some of the oscillators have the driving period and some the doubled

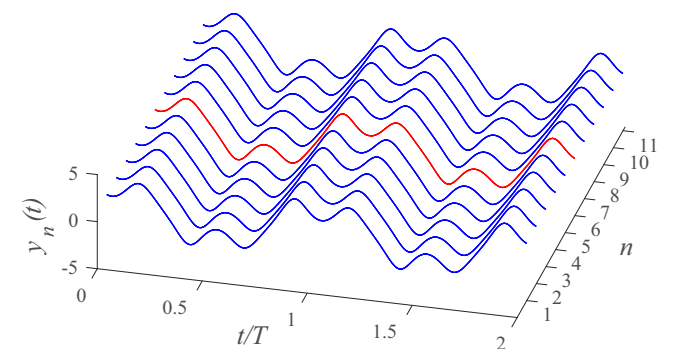


FIG. 7. The solutions of coupled driven oscillators with periodic boundary conditions. Initially, the middle oscillator oscillates with a doubled period while all others oscillate with the period of the driving force. Due to the strong coupling between the oscillators ($c = 1$), the middle oscillator converges to the same frequency as its neighbors, as expected.

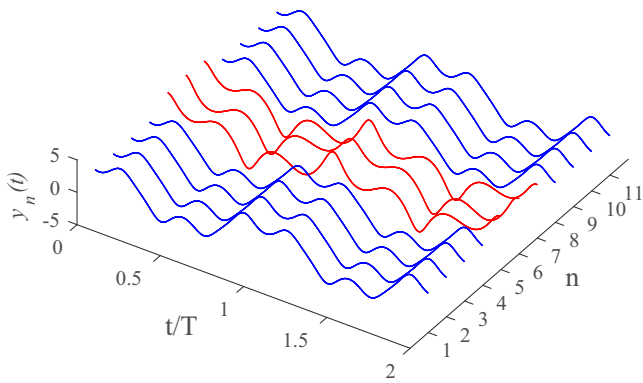


FIG. 8. A stable solution of coupled driven oscillators with periodic boundary conditions. The three middle oscillators oscillate with a doubled period while the other oscillators have the frequency of the driving force. The parameters are the same as in Fig. 2 with $c = 0.1$.

period) converges to a stable state with all oscillators having the driving period. For any initial mixed state, it is possible to find a weak enough coupling for which the mixed initial state remains with the same mixture of frequencies. For intermediate coupling strength, the system may converge to a complicated stable state similar to the one shown above (Figs. 5 and 6). Obviously, homogeneous initial states, in which each of the oscillators has the same stable state when uncoupled, remain stable due to the fact that the coupling term effectively vanishes.

The solutions shown above are not unique, and different combinations of oscillators with either a doubled period or the original period are possible (depending on the initial solution or on the perturbations applied to the system). To illustrate this, we show in Figs. 8 and 9 solutions in which the three or five middle oscillators have the doubled period while all the others have the period of the driving force.

For clarity, we present the power spectra of the coupled oscillators for these latter cases in Figs. 10 and 11. The spectra show that indeed the three or five middle oscillators have peaks for integer multiples of $\omega_0/2$ (corresponding to the

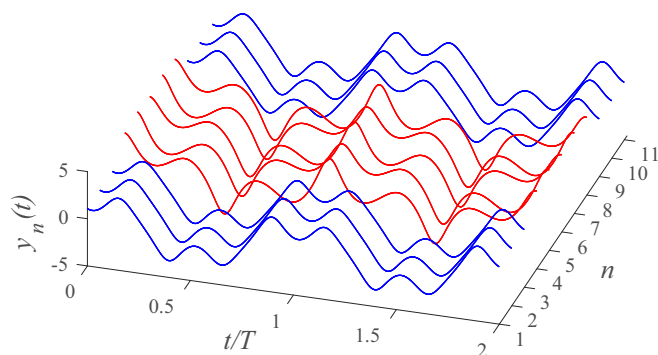


FIG. 9. A stable solution of coupled driven oscillators with periodic boundary conditions. The five middle oscillators oscillate with a doubled period while the other oscillators have the same frequency as the driving force. The parameters are the same as in Fig. 8.

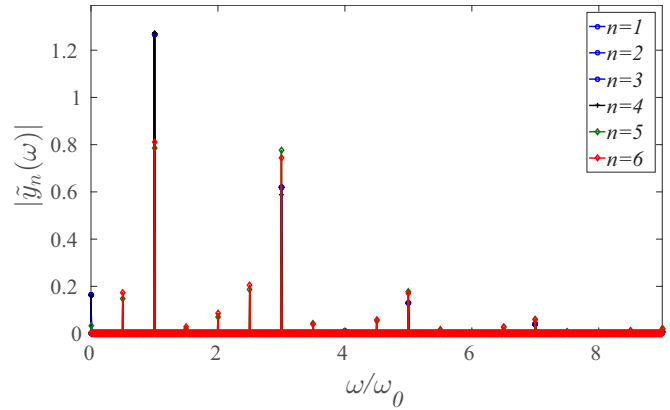


FIG. 10. The power spectra of coupled oscillators. The three middle oscillators ($n = 5-7$) show peaks at $\omega_0/2$ and some odd multiples of this frequency while the others (only $n = 1-4$ are shown) only show peaks at integer multiples of ω_0 . The parameters are the same as in Fig. 8.

doubled period), while the others have peaks only for integer multiples of the driving force frequency, ω_0 (corresponding to the period of the driving force).

In summary, the results presented here show that in a lattice of nonlinear oscillators, period-doubled oscillations can be locally maintained leading to the concept of a double-period breather. This phenomenon was already noted for a more complicated and specific model of double-stranded DNA and for a specific set of parameters [8,9]. However, the complexity of the physical model investigated there limits the ability to explore the mechanisms that allow the existence of these discrete breathers. Here, we used the simplest model for coupled nonlinear oscillators, a chain of linearly coupled Duffing-Helmholtz oscillators. This simple model has been used to study memory and logic devices [15,16], neural networks [17,18], the recurrence of Earth’s ice ages [20], piezoelectric buckled beams [21], and many other systems. Different aspects of the system were investigated, including the effect

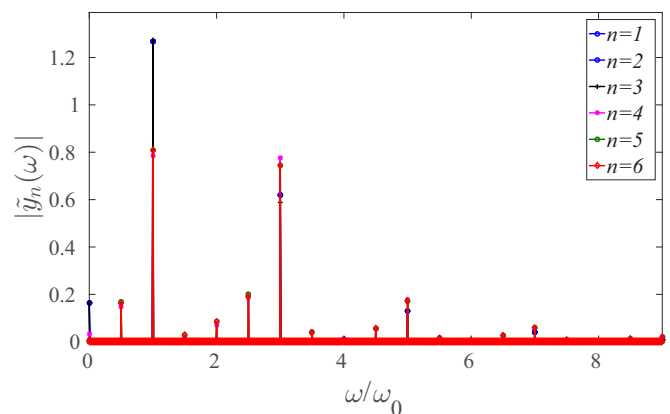


FIG. 11. The power spectra of coupled oscillators. The five middle oscillators ($n = 4-8$) show peaks at $\omega_0/2$ and some odd multiples of this frequency while the others (only $n = 1-3$ are shown) only show peaks at integer multiples of ω_0 . The parameters are the same as in Fig. 8.

of noise on the hysteresis of a single oscillator [22], the noise-induced intermittency of two coupled oscillators [23], chaos and routes to chaos [24,25], synchronization [26,27], and others. Here, using numerical continuation, we found the bifurcation diagram and identified a bistability region of oscillations with the driving period and with the doubled period. This information allowed us to find the range of coupling strengths for which some of the oscillators have the driving period while their neighbors have the doubled period. In particular, we found that, in the limit of weak coupling, the different oscillators may have different frequencies in the stable state, and in the limit of strong coupling, all the oscillators converge to the frequency of the driving force. For intermediate coupling, some of the oscillators effectively

experience non-monochromatic driving (the external force and neighbors do not oscillate with the same frequency) and, therefore, the stable state of the system is not a simple combination of oscillators with either the driving period or the doubled period, but rather oscillations with a complex spectra. We believe that our results may have implications for the dynamics of various physical systems described using models with discrete breather solutions.

This work was performed at the Los Alamos National Laboratory (LANL), operated by the Los Alamos National Security, LLC (LANS), under Contract No. DE-AC52-06NA25396 with the U.S. Department of Energy. G.B. thanks LANL for its hospitality during the work on this project.

-
- [1] S. Flach and C. R. Willis, *Phys. Rep.* **295**, 181 (1998).
 - [2] M. V. Ivanchenko, *Phys. Rev. Lett.* **102**, 175507 (2009).
 - [3] N. Boechler, G. Theocharis, S. Job, P. G. Kevrekidis, M. A. Porter, and C. Daraio, *Phys. Rev. Lett.* **104**, 244302 (2010).
 - [4] G. Theocharis, N. Boechler, P. G. Kevrekidis, S. Job, M. A. Porter, and C. Daraio, *Phys. Rev. E* **82**, 056604 (2010).
 - [5] N. Lazarides and G. P. Tsironis, *Phys. Rev. Lett.* **110**, 053901 (2013).
 - [6] M. Syafwan, H. Susanto, and S. M. Cox, *Phys. Rev. E* **81**, 026207 (2010).
 - [7] P. Maniadis and S. Flach, *Europhys. Lett.* **74**, 452 (2006).
 - [8] B. S. Alexandrov, V. Gelev, A. R. Bishop, A. Usheva, and K. Ø Rasmussen, *Phys. Lett. A* **374**, 1214 (2010).
 - [9] P. Maniadis, B. S. Alexandrov, A. R. Bishop, and K. Ø Rasmussen, *Phys. Rev. E* **83**, 011904 (2011).
 - [10] L. Q. English, F. Palmero, P. Candiani, J. Cuevas, R. Carretero-González, P. G. Kevrekidis, and A. J. Sievers, *Phys. Rev. Lett.* **108**, 084101 (2012).
 - [11] Y. Xu, T. J. Alexander, H. Sidhu, and P. G. Kevrekidis *Phys. Rev. E* **90**, 042921 (2014).
 - [12] F. Palmero, J. Han, L. Q. English, T. J. Alexander, and P. G. Kevrekidis, *Phys. Lett. A* **380**, 402 (2016).
 - [13] U. Parlitz and W. Lauterborn, *Phys. Lett. A* **107**, 351 (1985).
 - [14] T. Kalmar-Nagy and B. Balachandran, in *The Duffing Equation: Nonlinear Oscillators and Their Behaviour*, edited by I. Kovacic and M. J. Brennan (Wiley, New York, 2011), pp. 139–174.
 - [15] A. Yao and T. Hikiyara, *IEICE Electron. Express* **9**, 1230 (2012).
 - [16] A. Yao and T. Hikiyara, *Phys. Lett. A* **377**, 2551 (2013).
 - [17] S. Grossberg, *Neural Networks* **1**, 17 (1988).
 - [18] P. Hänggi, *Chem. Phys. Chem.* **3**, 285 (2002).
 - [19] E. J. Doedel, *Congr. Numer.* **30**, 265 (1981).
 - [20] R. Benzi, G. Parisi, A. Sutera, and A. Vulpiani, *Tellus* **34**, 10 (1982).
 - [21] F. Cottone, L. Gammaitoni, H. Vocca, M. Ferrari, and V. Ferrari, *Smart Mater. Struct.* **21**, 035021 (2012).
 - [22] E. Perkins, *Phys. Lett. A* **381**, 1009 (2017).
 - [23] S. Rajasekar, M. C. Valsakumar, and S. P. Raj, *Phys. A (Amsterdam, Neth.)* **261**, 417 (1998).
 - [24] A. Kenfack, *Chaos Solitons Fractals* **15**, 205 (2003).
 - [25] D. E. Musielak, Z. E. Musielak, and J. W. Benner *Chaos Solitons Fractals* **24**, 907 (2005).
 - [26] U. E. Vincent and A. Kenfack, *Phys. Scr.* **77**, 045005 (2008).
 - [27] D. H. Zanette, *Europhys. Lett.* **115**, 2009 (2016).